Numerical investigation of flow mixing in sinusoidal channels by using Lattice Boltzmann Method

Maedeh Asadi
Mechanical engineering department, Ferdowsi university of Mashhad, Mashhad, Iran
Maedeh.asadi@mail.um.ac.ir

Omid Reza Mohammadipour
Mechanical engineering department
Payame Noor university, Tehran, Iran
o.mohammadipour@pnu.ac.ir

Hamid Niazmand
Mechanical engineering department, Ferdowsi university of Mashhad, Mashhad, Iran
niazmand@um.ac.ir

Abstract

The purpose of this study is to investigate the mixing phenomena in a sinusoidal microchannel and call into question the effect of unequal wave length magnitude in the upper and lower walls on mixing efficiency. Nondimensional parameters in this study were Schmidt number set to remain at 100, Reynolds number ranging from 0.5 to 1.5 and different wave length ratio values for lower wall, while the upper wall wave length was invariant. To answer this question, all governing equations are solved numerically using the lattice Boltzmann method, while channel walls are modelled by the aid of a general curved boundary treatment. This analysis revealed that corrugated patterns led to higher pressure drop and preferable mixing efficiency at lower distance from the beginning of the channel. Interestingly, results showed that the mixing efficiency decreases as the Reynolds number increases. The evidence from this research intimates that almost complete mixing (up to 98 %) was achieved at Peclet=50 at the outlet of the channel in which the dimensionless wave length magnitude for the upper and lower walls are equal to 3 and 4 respectively. A pressure drop of 277 Pa is obtained for this case.

Key words: Mixing efficiency, sinusoidal channels, Lattice Boltzmann Method, Microchannel.

1. Introduction

This research constitutes a relatively new area, which has emerged from wavy channels utilization in microchannels. There are growing appeals for sinusoidal channels in passive micromixers which enhance mixing by increasing contact interfaces between species [1]. Not only these corrugated channels are applied in confined sinusoidal jets [2], but also they are widely exploited in microchannel heat sinks for electrical cooling [3]. Therefore, significant studies have been carried out on these patterns recently. Oviedo-Tolentino et al. [4] examined the entrance part of a sinusoidal channel and found that at least eight waves must be applied to obtain appropriate flow distribution in their case of study.

This phenomenon has been widely investigated by Sui et al. [5] in a three-dimensional channel. They proposed that fluid mixing enhancement in wavy microchannels is due to the production of secondary flow or Dean vortices and chaotic advection occurrence because of replacement of vortices along flow direction. For further review on Dean vortices role in mixing

enhancement, Khosravi Parsa et al. [6] employed a sinusoidal passive micromixer and they concluded that this effect only is important in high Reynolds numbers while for low Reynolds numbers, diffusion is the only factor of mixing. Solehati et al. [7] accomplished mixing in a T-shape wavy micro channel and reported better mixing index compared with its plain familiar paradigm. They stated the chaotic flow regime caused from secondary flow in curved areas, helped the mixing phenomena.

One of the major topics to be investigated for flow characteristics in wavy channels, are estimating the main effective geometry parameters. Khoshvaght-Aliabadi[8] used SIMPLE algorithm to study flow characteristics of sinusoidal-corrugated channels and concluded that among design parameters, wave amplitude and wave length had the highest effect on Darcy friction factor. Akbarzadeh et al.[9] modeled three types of corrugated surfaces including triangular, trapezoidal and sinusoidal in wavy channels. They reported an increasement in pressure drop in comparison with plain channel but altogether among these profiles sinusoidal wall was suggested owing to higher performance and lower entropy generation. Dormohammadi et al.[10] carried out a simulation of nanofluid heat transfer and entropy generation in sinusoidal channel. They reported that at wave length ratio of 1 and wave amplitude ratio of 0.2 the optimal design can be achieved.

A finite volume method has been recently used to investigate the phase difference effect on mixing efficiency. The results showed that asymmetric channels have better mixing efficiency than their symmetric counterparts as they produce periodic circular patterns [11]. Mondal et al. conducted a numerical study using finite element method on flow mixing in racoon and serpentine micromixers. They reported that racoon mixer has better mixing efficiency in comparison with serpentine. On the other hand, its pressure drop is higher than serpentine one and in general due to the lowest mixing cost in serpentine mixer , it can be adapted as the best design [12].

Nakhchi [13] performed an experiment to investigate geometric and flow parameters effect on pressure drop and thermal performance of sinusoidal channels. He concluded that among geometric and flow parameters, the wave's amplitude aspect ratios and Reynolds number have more influence on heat transfer enhancement and pressure drop, respectively. Ahmadpour and Noori Rahim Abadi [14] considered a vertical wavy channel to study heat transfer and pressure drop of multiphase flows. They discovered that the use of wavy channels was rational for low mass fluxes with phase shift angle of 180 degree.

In particular no study, to our knowledge, has considered the effect of inequivalent wave length ratios on both side of the walls of the channel to simulate flow and mixing efficiency of the flow by use of Lattice Boltzmann Method (LBM). Here LBM technique have been developed to solve the problem. The objective is to demonstrate the feasibility of corrugating channel walls in order to approach mixing efficiency enhancement in low ranges of Reynolds numbers.

2. Problem Definition and Governing Equations

To take into account the influence of unequal wave length on mixing enhancement, four different wave length values for the lower wall have been selected, while the upper wall wave length is invariant in all cases. A plain channel with no corrugated pattern is also considered as a reference case. Achieving desired mixing at the outlet of the microchannels requires a relatively long length due to low Re numbers. Considering the Hight of the channel at the inlet to be D, the entire length of the channel is set to be 26 D. Channel walls are following the sinusoidal functions as follows:

$$y = \begin{cases} D\left(\frac{1}{2} + 0.25\sin\left(\frac{2\pi}{3D}(x-D)\right)\right) & : upper\ wall \\ D\left(\frac{1}{2} + 0.25\sin\left(\frac{2\pi}{\lambda D}(x-D)\right)\right) & : lower\ wall \end{cases} \qquad D < x < 25D \tag{1}$$

(2)

Lower wall wave length number (λ) is set to be 1,2,3 and 4, thus different patterns of corrugate channels are obtained. In simulations D is chosen to be 30 μm and Fig. 1 shows the geometry of channel for or λ=1. This curved complex design is drawn by the aid of cloud input method which had been represented in Ref. [15].

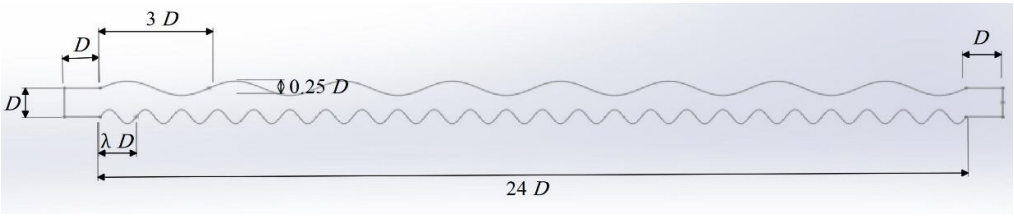

Fig. 1. Schematic of sinusoidal micromixer for λ=1.

Assuming $\vec{V}, \mathrm{P}, \mathrm{C}$ as velocity vector, pressure and concentration, respectively, the well-known Navier-Stokes equations and Advection-Diffusion equation are implemented to solve steady incompressible fluid flow and concentration as follows[16] :

$$\vec{\nabla}.\vec{V} = 0 \tag{3}$$

$$\rho(\vec{V}.\vec{\nabla})\vec{V} = -\vec{\nabla}P + \mu\nabla^2(\vec{V}) \tag{4}$$

$$\vec{V}.\vec{\nabla}C = D_c\nabla^2 C \tag{5}$$

In above equations ρ is density, μ is dynamic viscosity and D_c is Species diffusivity coefficient. It is possible to write nondimensionalized equations by assuming these parameters:

$$X^* = \frac{x}{H}, y^* = \frac{y}{H}, \overrightarrow{V^*} = \frac{\vec{V}}{U_{ref}}, P^* = \frac{P}{\rho U_{ref}^2}, C^* = \frac{C}{C_0} \tag{6}$$

The dimensionless equations can be achieved by omitting the superscripts as follows[17]:

$$\vec{V}.\vec{\nabla}(\vec{V}) = -\vec{\nabla}P + \frac{1}{Re}\nabla^2(\vec{V}) \tag{7}$$

$$\vec{V}.\vec{\nabla}C = \frac{1}{Re.Sc}\nabla^2 C \tag{8}$$

In above equations, $Re = \rho U_{ref} H/\mu$ is the Reynolds number and $Sc = \mu/\rho D_c$ is the Schmidt number for the concentration distribution. These equations are corresponded to the following boundary conditions:

$$Wall: \begin{cases} \vec{V} = 0 \\ \vec{\nabla} C . \overrightarrow{n_{\perp}} = 0 \end{cases} \tag{9}$$

$$inlet: \begin{cases} \vec{V} = U_{inlet} \\ C = \begin{cases} 0 & 0 < y < H/2 \\ 1 & H/2 < y < H \end{cases} \end{cases} \tag{10}$$

$$outlet: \begin{cases} \frac{\partial u}{\partial x} = 0 \\ \frac{\partial C}{\partial x} = 0 \end{cases} \tag{11}$$

The mixing performance of two fluids (ε_m) is evaluated at any cross section as[18] :

$$\varepsilon_m = 1 - \frac{1}{H}\int_0^H \left|\frac{C(y) - C_\infty}{C_0 - C_\infty}\right| dy \tag{12}$$

Where C_0 and C_∞ are concentration at the inlet and fully mixed conditions. The value of ε_m varies from 0 for fully unmixed to 1 for mixed state respectively.

3. Numerical Method

Aforesaid equations are solved numerically by the use of lattice Boltzmann method. Owing to the fact that LBM simulation has the capability of being parallelized, collision and streaming steps can be incorporated in order to decrease the time to solve the problem[19].

3.1. LBM For Flow Field

By considering $f(r,t)$ as the distribution function at a given location r and time t , the single-relaxation-time BGK model can be implemented to simulate fluid flow [20] :

$$f_i(r + c_i\delta t, t + \delta t) = f_i(r,t) + \frac{1}{\tau_f}\left(f_i^{eq}(r,t) - f_i(r,t)\right) \tag{13}$$

Where δt is time step and c_i is the mesoscopic velocity in i-direction. The D2Q9 model with these discrete velocity set is adopted in this work:

$$\begin{cases} c_0 = (0,0) \\ c_i = (\cos\theta, \sin\theta)c, & \theta = \frac{(i-1)\pi}{2}, \quad i = 1-4 \\ c_i = \sqrt{2}(\cos\theta, \sin\theta)c, & \theta = \frac{(i-1)\pi}{2} + \frac{\pi}{4}, \quad i = 5-8 \end{cases} \tag{14}$$

$c = \frac{\delta x}{\delta t}$ is lattice speed and δx is lattice spacing. τ_f which is called the dimensionless relaxation time can be obtained from Re as $\tau_f = \frac{3}{Re}\frac{\delta t}{\delta x^2} + \frac{1}{2}$.

For nearly incompressible flow f_i^{eq} is estimated by Maxwell-Boltzmann equilibrium distribution function as follows:

$$f_i^{eq} = w_i \rho \left[1 + \frac{\vec{c_i}.\vec{V}}{c_s^2} + \frac{(\vec{c_i}.\vec{V})^2}{2c_s^4} - \frac{\vec{V}^2}{2c_s^2}\right] \tag{15}$$

$$w_i = \begin{cases} 4/9 & \alpha = 0 \\ 1/9 & \alpha = 1-4 \\ 1/36 & \alpha = 5-8 \end{cases} \tag{16}$$

$c_s^2 = c^2/3$ is the sound speed of the model. The local macroscopic variables, such as density, velocity and pressure are statistically calculated from f_i using:

$$\rho = \sum_i f_i \tag{17}$$

$$\vec{V} = \frac{1}{\rho}\sum_i f_i \vec{c_i} \tag{18}$$

$$P = \rho c_s^2 \tag{19}$$

3.2. LBM For Concentration Field

The evolution equation to solve advection-diffusion equation can be described as [21]:

$$j_i(r + c_i\delta t, t + \delta t) = j_i(r,t) + \frac{1}{\tau_j}\left(j_i^{eq}(r,t) - j_i(r,t)\right) \tag{20}$$

$$j_i^{eq} = w_i C\left[1 + \frac{\vec{c_i}.\vec{V}}{c_s^2} + \frac{\left(\vec{c_i}.\vec{V}\right)^2}{2c_s^4} - \frac{\vec{V}^2}{2c_s^2}\right] \tag{21}$$

In above equation $\tau_j = \frac{3}{Re.Sc_c}\frac{\delta t}{\delta x^2} + \frac{1}{2}$ is the nondimensional relaxation time and related to Peclet number($Pe = Re.Sc_c$)while the macroscopic concentration of flow can be evaluated by:

$$C = \sum_i j_i \tag{22}$$

3.3. LB Boundary Conditions

For flow field, general boundary treatment for velocity which has been introduced for the first time by the present authors in Ref. [22], is applied at inlet and outlet of the channel. More significantly for the curved boundaries on side walls, general curved boundary treatment is used. Anyone interested in the frame work, may refer to the authors previous work [15].To illustrate how macroscopic values on curved boundaries like R_1 will be obtained from two fluid nodes in this method (R_2, R_3),the scheme of the extrapolation is shown in Fig. 2.

3.4. Validation and Grid Independency

For grid independency at Pe=50, plain channel with different nodes in y direction were taken on and mixing efficiency at the inlet is reported in Table. 1. Reference number of nodes for LBM is set to be 31 to reduce computational costs and enough precision.

Table 1. variation of ε_m at different number of nodes at Pe=50 for plain channel

Number of nodes	11	21	31	41
ε_m	0.873043479	0.939729104	0.960687471	0.97097258

Toward validating the method, flow mixing between two parallel plate was simulated and concentration values at any points of the region was evaluated relative to analytical solution presented by Wu and Nguyen [23]. It is noticeable that, however, in theoretical solution the y momentum component is taken zero, in our work it is taken into account. Fig. 3 displays the values obtained from analytical solution and the results obtained in this study. With respect to above subject, the results had the maximum 0.05 difference with each other.

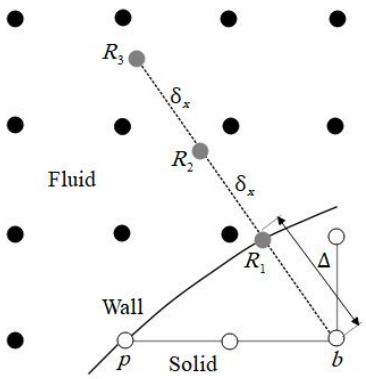

Fig. 2. Layout of three reference points (R_1, R_2, R_3) for the boundary nod (b)

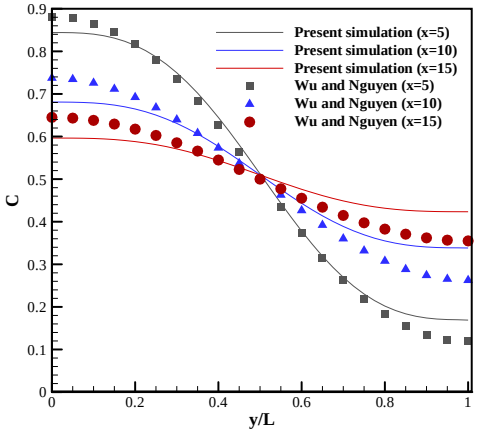

Fig. 3. Comparison between concentration (C) values at different cross sections for presented study and Wu analytical solution at Pe=100

4. Results and Discussion

We start describing our findings by concentration contours and streamlines for different patterns of channels shown in Fig. 4. In order to have a better close up of vortices and streamlines only 15 units of the channel length are zoomed in. These contours demonstrate two things. First, mixing phenomenon occurs earlier in wavy channels than plain channel. Second, flow transmission affects directly on mixing. As can be seen from the figure, channel with lower wall wave length equal to one, some vortices were made in corrugated parts, so mixing length was less than other patterns.

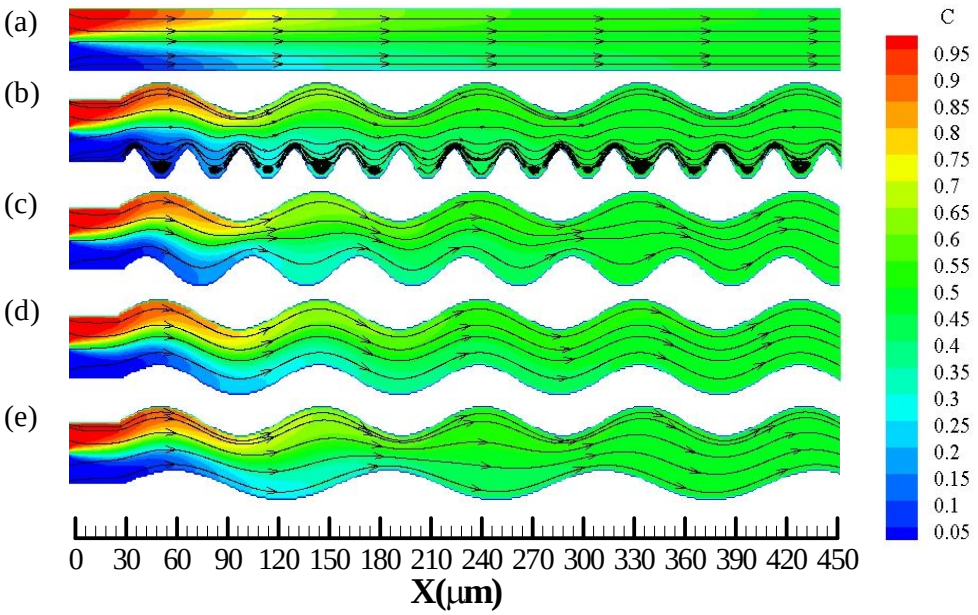

Fig. 4. Streamlines and concentration (C) field at Re=1, Sc=100 for different geometry patterns: a) plain channel, b) lower wall λ=1, c) lower wall λ=2, d) lower wall λ=3 and e) lower wall λ=4channel

A better understanding of mixing efficiency along the channel in different cross sections, can be obtained by Fig. 5 in which the mixing efficiency is depicted according to distance from inlet. For lower wall wave length number equivalent to one, better mixing happened at only 0.4 length of the entire channel, however, channel with wave length number of 4 units, achieved better mixing efficiency at the outlet of the channel. In all Reynolds numbers mixing was enhanced along the channel and according to this figure, from 0.7 distance of the entire channel length the mixing efficiency is approximately constant which shows enough length for mixing. It is also observed that for all Reynolds numbers, mixing efficiency at the outlet of the all channels were nearly the same, but with corrugated pattern, shorter mixing length could be implied nonetheless.

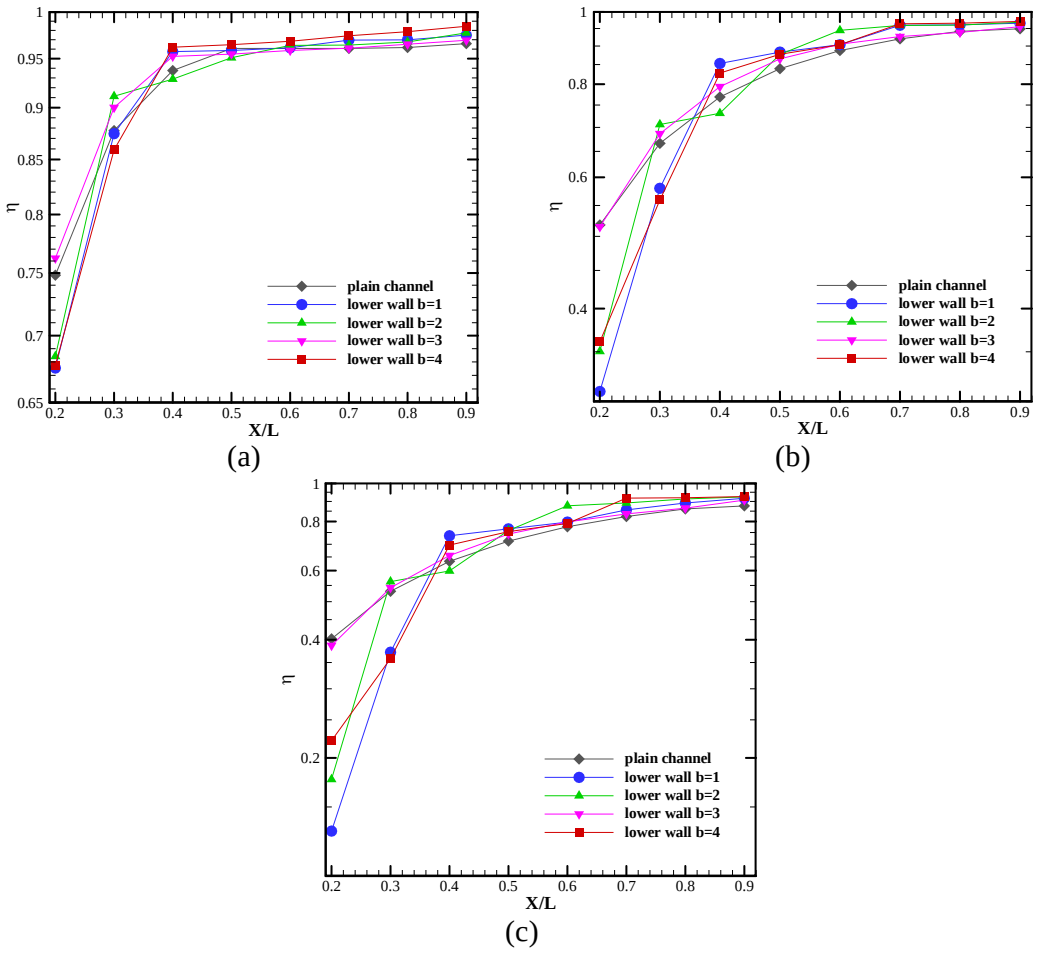

Fig. 5. Mixing efficiency variations along the channel for different geometries at Sc=100 and different Reynolds number: (a) Re=0.5, (b) Re=1.0, (c) Re=1.5.

So far, sinusoidal channels led to good results, even if the improvement was negligible. Another promising finding was that increasing Re caused in mixing efficiency reduction and pressure drop augmentation. The results are indicated in Fig. 6. A similar pattern of results was obtained in Ref. [12] in which higher Re numbers were investigated. Before explaining the figures, it should be noted that the approach utilized suffers from limitation that we are not able

to choose any desired Peclet numbers, due to the fact that the convergency of method is highly affected by the dimensionless relaxation time parameter which depends on Peclet number.

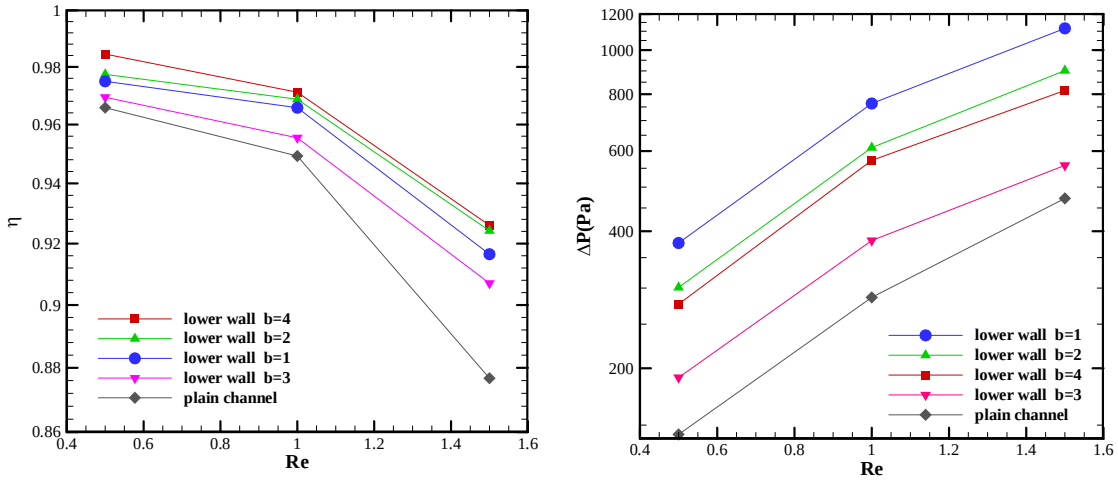

(a) (b)

Fig. 6. Effect of Reynolds increment on: (a) mixing efficiency, (b) pressure drop at Sc=100

There were also significant consequences for increasing Re. The more Re values we have, the more prompt the flow moves and therefore flow particles are not able to repose and mix together which lead to decreasing in mixing efficiency. Determining the appropriate pattern also is taken effect of pressure drop. As can be discerned from Fig. 6.b lower wall wave length number of 1 unit had much higher pressure drop due to vortices made in hollow parts as mentioned already, where as plain channel had the least in all Re. Also, it is apperceived that higher Re had caused more recirculation of flow and hence the pressure drop arose.

Having investigated both pressure difference and mixing efficiency along the entire channel, sinusoidal walls with different wave length magnitude equal to 3 at the top and 4 at the bottom offers better mixing efficiency equal to 0.98 which is near to complete mixing and pressure drop of 277 Pa at Re=0.5. Nonetheless, we believe that it is well justified to mention this low Reynolds number will increase the time of the process because the flow moves so slowly.

5. Conclusions

In conclusion, it would appear that the Lattice Boltzmann method which has been carried out in this research can successfully simulate mixing flow in complex geometries such as sinusoidal channels. The analysis leads to the following conclusions:

- Diminution of mixing efficiency and amplification of pressure drop were observed while raising Re from 0.5 to 1.5 for $Sc = 100$.
- Almost 0.7 of the total length of channel was required to obtain mixing reported at the outlet of the channel.
- Selection of different wave length for up and down sinusoidal walls can amend mixing efficiency. The channel with wave length corresponded to dimensionless values of three

at the top and four at the bottom reported 98 percent with pressure drop of 277 Pa at Re=0.5.

Despite the limitations these results are valuable in light of utilizing this method at low Peclet numbers for microchannels for even modeling other flow characteristics such as heat transfer or electroosmotic flows which may constitute the subject of future studies.

References

[1] Chen, C.o.-K. and C.-C. Cho, 2007, Electrokinetically-driven flow mixing in microchannels with wavy surface, Journal of Colloid and Interface Science, vol **312**(2), pp 470-480.

[2] Rahimi-Esbo, M., et al., 2012, Numerical study of turbulent forced convection jet flow in a converging sinusoidal channel, International Journal of Thermal Sciences, vol **59**, pp 176-185.

[3] Xie, G., et al.,2013, Comparative Study of Thermal Performance of Longitudinal and Transversal-Wavy Microchannel Heat Sinks for Electronic Cooling, Vol. **135**, 021008.

[4] Oviedo-Tolentino, F., et al.,2008, Experimental study of fluid flow in the entrance of a sinusoidal channel, International Journal of Heat and Fluid Flow, vol **29**(5), pp 1233-1239.

[5] Sui, Y., et al.,2010, Fluid flow and heat transfer in wavy microchannels, International Journal of Heat and Mass Transfer, vol **53**(13), pp 2760-2772.

[6] Khosravi Parsa, M., F. Hormozi, and D. Jafari, 2014, Mixing enhancement in a passive micromixer with convergent–divergent sinusoidal microchannels and different ratio of amplitude to wave length, Computers & Fluids, vol **105**, pp 82-90.

[7] Solehati, N., J. Bae, and A.P. Sasmito,2014, Numerical investigation of mixing performance in microchannel T-junction with wavy structure, Computers & Fluids, vol **96**, pp 10-19.

[8] Khoshvaght-Aliabadi, M., 2014, Influence of different design parameters and Al2O3-water nanofluid flow on heat transfer and flow characteristics of sinusoidal-corrugated channels, Energy Conversion and Management, vol **88**, pp 96-105.

[9] Akbarzadeh, M., S. Rashidi, and J.A. Esfahani, 2017, Influences of corrugation profiles on entropy generation, heat transfer, pressure drop, and performance in a wavy channel, Applied Thermal Engineering, vol **116**, pp 278-291.

[10] Dormohammadi, R., et al.,2018, Heat transfer and entropy generation of the nanofluid flow inside sinusoidal wavy channels, Journal of Molecular Liquids, vol **269**, pp 229-240.

[11] Borgohain, P., et al.,2018, Numerical investigation of mixing enhancement for multi-species flows in wavy channels, Chemical Engineering and Processing - Process Intensification, vol **127**, pp 191-205.

[12] Mondal, B., et al., 2019, Numerical study of mixing in wavy micromixers: comparison between raccoon and serpentine mixer, Chemical Engineering and Processing - Process Intensification, vol **136**, pp. 44-61.

[13] Nakhchi, M.E., 2019, Experimental optimization of geometrical parameters on heat transfer and pressure drop inside sinusoidal wavy channels, Thermal Science and Engineering Progress, vol **9**, pp 121-131.

[14] Ahmadpour, A. and S.M.A. Noori Rahim Abadi, 2019, Thermal-hydraulic performance evaluation of gas-liquid multiphase flows in a vertical sinusoidal wavy channel in the presence/absence of phase change, International Journal of Heat and Mass Transfer, vol **138**, pp 677-689.

[15] Mohammadipour, O., S. Succi, and H. Niazmand, 2018, General curved boundary treatment for two- and three-dimensional stationary and moving walls in flow and nonflow lattice Boltzmann simulations, Physical Review E. **98**, 23304.

[16] Khozeymeh-Nezhad, H. and H. Niazmand, 2018, A double MRT-LBM for simulation of mixing in an active micromixer with rotationally oscillating stirrer in high Peclet number flows, International Journal of Heat and Mass Transfer, vol **122**, pp 913-921.

[17] Basati, Y., O.R. Mohammadipour, and H. Niazmand, 2019, Numerical investigation and simultaneous optimization of geometry and zeta-potential in electroosmotic mixing flows, International Journal of Heat and Mass Transfer, vol **133**, pp 786-799.

[18] Kazemi, S., et al., 2017, Two dimensional numerical study on mixing enhancement in micro-channel due to induced charge electrophoresis, Chemical Engineering and Processing - Process Intensification, vol **120**, pp 241-250.

[19] Basha, M. and N.A.C. Sidik, 2018, Numerical predictions of laminar and turbulent forced convection: Lattice Boltzmann simulations using parallel libraries, International Journal of Heat and Mass Transfer,vol **116**, pp 715-724.

[20] Qian, Y.H., D. D'Humières, and P. Lallemand, 1992, Lattice BGK Models for Navier-Stokes Equation. Europhysics Letters (EPL), vol **17**(6), pp 479-484.

[21] Fu, Y., et al., 2018, Simulation of reactive mixing behaviors inside micro-droplets by a lattice Boltzmann method. Chemical Engineering Science, vol **181**, pp 79-89.

[22] Mohammadipour, O., H. Niazmand, and S. Succi, 2017, General velocity, pressure, and initial condition for two-dimensional and three-dimensional lattice Boltzmann simulations. Vol. 95.

[23] Wu, Z. and N.-T. Nguyen, 2005, Convective–diffusive transport in parallel lamination micromixers, Vol. **1**, pp 208-217.